OPEN

Characterization of Myocardial Microstructure and Function in an Experimental Model of Isolated Subendocardial Damage

Niklas Beyhoff, David Lohr, Anna Foryst-Ludwig, Robert Klopfleisch, Sarah Brix, Jana Grune, Arne Thiele, Lasti Erfinanda, Arata Tabuchi, Wolfgang M. Kuebler, Burkert Pieske, Laura M. Schreiber, Ulrich Kintscher

Abstract—Subendocardial damage is among the first cardiac manifestations of hypertension and is already present in asymptomatic disease states. Accordingly, markers of subendocardial impairment may facilitate early detection of cardiac damages and risk stratification under these conditions. This study aimed to investigate the impact of subendocardial damage on myocardial microstructure and function to elucidate early pathophysiologic processes and to identify corresponding diagnostic measures. Mice (n=38) were injected with isoproterenol to induce isolated subendocardial scarring or saline as corresponding control. Cardiac function and myocardial deformation were determined by high-frequency echocardiography. The cardiac stress response was assessed in a graded exercise test and during dobutamine stress echocardiography. Myocardial microstructure was studied ex vivo by 7 T diffusion tensor magnetic resonance imaging at a spatial resolution of 100×100×100 µm^3. Results were correlated with histology and biomarker expression. Subendocardial fibrosis was accompanied by diastolic dysfunction, impaired longitudinal deformation (global peak longitudinal strain [LS]: −12.5±0.5% versus −15.6±0.5%; P<0.001) and elevated biomarker expression (ANP [atrial natriuretic peptide], Galectin-3, and ST2). Systolic function and cardiac stress response remained preserved. Diffusion tensor magnetic resonance imaging revealed a left-shift in helix angle towards lower values in isoproterenol-treated animals, which was mainly determined by subepicardial myofibers (mean helix angle: 2.2±0.8° versus 5.9±1.0°; P<0.01). Longitudinal strain and subepicardial helix angle were highly predictive for subendocardial fibrosis (sensitivity, 82%–92% and specificity, 89%–90%). The results indicate that circumscribed subendocardial damage alone can cause several hallmarks observed in cardiovascular high-risk patients. Microstructural remodeling under these conditions involves also remote regions, and corresponding changes in longitudinal strain and helix angle might serve as diagnostic markers. **(*Hypertension*. 2019;74:295-304. DOI: 10.1161/HYPERTENSIONAHA.119.12956.)** ● **Online Data Supplement**

Key Words: diffusion tensor magnetic resonance imaging ■ myocardial strain; remodeling ■ speckle tracking ■ subendocardium

The subendocardium is the innermost myocardial layer and is highly vulnerable against injury.[1] Therefore, the subendocardium is often considered the myocardial layer affected first in many cardiac diseases.[1] Experimental data indicate that adverse remodeling in response to multiple cardiovascular risk factors starts in the subendocardium of the left ventricle (LV) before occurring in other myocardial layers.[2–5] Hypertension and concomitant cardiac hypertrophy are accompanied by abnormal coronary autoregulation and consequently reduced perfusion pressure in the subendocardium, which may predispose to subendocardial ischemia.[6,7] Recently, Ishizu et al[2] demonstrated that subendocardial fibrosis is among the first cardiac manifestations of hypertension preceding functional changes. Accordingly, diagnostic markers of subendocardial status may facilitate early detection of cardiac damages and risk stratification already in asymptomatic disease states. Despite accepted clinical surrogates of subendocardial function such as global peak LS,[8] however, multiple confounding factors hamper the

Received March 6, 2019; first decision March 26, 2019; revision accepted May 12, 2019.

From the Charité—Universitätsmedizin Berlin, corporate member of Freie Universität Berlin, Humboldt-Universität zu Berlin, and Berlin Institute of Health, Institute of Pharmacology, Center for Cardiovascular Research, Berlin, Germany (N.B., A.F.-L., S.B., J.G., Arne Thiele, U.K.); DZHK (German Centre for Cardiovascular Research), Partner site Berlin, Germany (N.B., A.F.-L., S.B., J.G., Arne Thiele, L.E., Arata Tabuchi, W.M.K., B.P., U.K.); Chair of Cellular and Molecular Imaging, Comprehensive Heart Failure Center (CHFC), University Hospital Wuerzburg, Germany (D.L., L.M.S.); Department of Veterinary Pathology, College of Veterinary Medicine, Freie Universität Berlin, Germany (R.K.); Charité—Universitätsmedizin Berlin, corporate member of Freie Universität Berlin, Humboldt-Universität zu Berlin, and Berlin Institute of Health, Institute of Physiology, Berlin, Germany (J.G., L.E., Arata Tabuchi, W.M.K.); and Department of Internal Medicine and Cardiology, Campus Virchow Klinikum, Charité—Universitätsmedizin Berlin and Deutsches Herzzentrum Berlin (DHZB), Department of Cardiology, Berlin, Germany (B.P.).

The online-only Data Supplement is available with this article at https://www.ahajournals.org/doi/suppl/10.1161/HYPERTENSIONAHA.119.12956.

Correspondence to Ulrich Kintscher, MD, Institute of Pharmacology, Center for Cardiovascular Research, Charité—Universitaetsmedizin Berlin, Hessische St 3–4, 10115 Berlin, Germany. Email ulrich.kintscher@charite.de

establishment of cause-effect relationships between subendocardial pathologies and diagnostic measures in humans and many animal models.

Several cardiac pathologies have been shown to alter the 3-dimensional arrangement of myofibers in the heart.[9–11] Within the normal LV, the myofibers form 2 counter-directional helices varying continuously in orientation (helix angle [HA]) from subendocardium (right-handed helix, positive HA) to subepicardium (left-handed helix, negative HA).[12] The integrity of this microstructural organization is a critical determinant of the mechanical properties of the LV, and disturbance of myofiber geometry may thus result in impaired cardiac function.[13] Diffusion tensor magnetic resonance imaging (DT-MRI) is a feasible tool to study the cardiac myofiber arrangement and has been applied in a variety of pathological conditions in humans as well as in animal studies.[9,10,14–16] However, there is a lack of data regarding the impact of subendocardial damage on myofiber organization and corresponding functional consequences.

In the present study, we aimed to characterize myocardial microstructure and function in an experimental model providing the opportunity to study isolated subendocardial fibrosis in the absence of major confounders like cardiac hypertrophy or altered loading conditions.[17] By combining comprehensive DT-MRI analyses with several measures available in patients, we sought to provide translational evidence for clinical observations. We hypothesized that subendocardial fibrosis (1) affects the myofiber arrangement in the LV; (2) leads to impaired cardiac function; and (3) is detectable by assessment of corresponding microstructural and functional changes.

Methods

The authors declare that all supporting data are available within the article and in the online-only Data Supplement. All in vivo experiments were approved by local authorities (Landesamt für Gesundheit und Soziales Berlin, Germany) and were conducted in accordance with the German Law on the protection of animals. All animals were kept in a 12 hour light/dark cycle and received standard diet ad libitum.

Study Protocol

Subendocardial damage was induced by subcutaneous injection of isoproterenol as described previously.[17,18] Male 129/Sv mice (6–8 weeks old; Janvier Labs, France) were treated for 4 consecutive days with either isoproterenol (n=20; 25 mg/kg; dissolved in saline) or saline as corresponding control (n=18, matched for weight). During the week after final treatment, exercise capacity was assessed by a graded exercise test protocol. After echocardiographic examination (including speckle-tracking echocardiography and dobutamine stress echocardiography) an additional week later, mice were euthanized, and tissues were harvested for further analyses. Hearts were sent to the MRI site (Comprehensive Heart Failure Center, University Hospital Wuerzburg, Germany) for high-resolution DT-MRI measurements in a 7 T scanner at a spatial resolution of 100×100×100 μm^3. Results were correlated with histology and gene expression analyses.

Detailed Methodology

The online-only Data Supplement contains detailed information on echocardiography, the graded exercise test protocol, tissue processing, DT-MRI measurements, histology, gene expression analyses, and statistics.

Results

One animal died after the third isoproterenol-application by reasons not further investigated; another isoproterenol-treated animal developed signs of myocardial infarction (ventricular aneurysm and impaired ejection fraction) and was, therefore, excluded from study results. All control animals finished the study protocol.

Gravimetric Measures and Cardiac Tissue Analyses

Weight development and final body weights were comparable between both groups (Table). No signs of cardiac hypertrophy or lung congestion were found during necropsy, as evident from indexed heart weights and lung wet/dry weight ratios, respectively (Table).

Isoproterenol-treated animals developed pronounced fibrotic lesions in the subendocardium, whereas subepicardial collagen content was similar in both groups (Figure 1A–1C). The degree of subendocardial fibrosis varied between the different cardiac segments (Figure S1 in the online-only Data Supplement) and was found to be highest at the apex of the LV (Figure 1D). Immunohistochemical analyses revealed the presence of $CD68^+$ macrophages within fibrotic lesions, which showed a comparable distribution pattern accordingly (Figure S2).

ANP (atrial natriuretic peptide) mRNA levels were significantly upregulated in the LV after treatment with isoproterenol (Figure 1E). These animals also showed a higher expression of genes involved in inflammation and extracellular matrix turnover, such as CD68, Galectin-3, and precursors of collagen I and III (Figure 1E). GDF15 (growth/differentiation factor 15) was not induced at this time point (Figure 1E). ST2 (interleukin 1 receptor-like 1) levels were significantly upregulated in isoproterenol-treated animals (Figure 1E).

Diffusion Metrics

DT-MRI parameters were assessed for each myocardial layer (subendocardium/subepicardium) and segment (base/mid/apex), or globally for the transmural myocardium and the whole LV (Figure 2A; Figure S3A). Animals with subendocardial fibrosis displayed significantly lower transmural and subendocardial mean diffusivity (MD; Figure 2B and 2C). Subepicardial MD decreased significantly at apex level only (Figure 2B and 2C). Fractional anisotropy (FA) did not differ between both groups in any layer or segment, although variability of FA values decreased after treatment with isoproterenol (Figure 2D; Figure S3B). All eigenvalues of the diffusion tensor were consistently lowered in the apical subendocardium only (Figure S3C–S3E).

Myofiber Arrangement

Myocardial microstructure was studied by 3-dimensional reconstruction of fiber tracts with respect to layer and segment (Figure 3). Both treatment groups showed the stereotypic arrangement of myofibers forming 2 counter-directional helices as illustrated in Figure 3A and 3B. Animals presenting with subendocardial damage showed a left-shift of HA in the LV towards more negative values (Figure 3C). On segmental level, this left-shift reached statistical significance at the apex region only (Figure S4). Analyses of the HA gradient across the myocardial wall revealed lower HAs in the meso-subepicardium of animals with subendocardial fibrosis (Figure 3D). This effect was present in all myocardial segments (Figure S4). Layer-specific analyses indicated that the observed left-shift was caused by a change of subepicardial HA towards steeper angles, whereas HAs in the subendocardium were comparable in all segments (Figure 3E). The reduction of subepicardial HA was evident in all myocardial segments (Figure 3E).

Cardiac Function

Ejection fraction and other parameters of global systolic function remained unchanged after isoproterenol-treatment (Table). Subendocardial fibrosis was accompanied by signs of diastolic dysfunction (Figure 4A); animals had prolonged isovolumic relaxation times (**$P<0.01$) and tended to have slower late filling rates in the transmitral flow profile ($P=0.07$; Table). Deceleration time of the early diastolic filling rate (E) was longer; however, differences did not reach statistical significance ($P=0.07$; Table). Early diastolic mitral annular velocity (e′) was lower (**$P<0.01$) leading to a reverse

Table. End Point Characteristics

Parameter	Control	Isoproterenol	*P* Value
Physiological data			
BW, g	26.2±0.4	26.7±0.3	0.36
ΔBW, %	+7.8±1.1	+9.1±1.0	0.40
Heart rate, bpm	370±7	347±11	0.10
Necropsy data			
Heart weight, mg	189±13	172±13	0.37
Heart weight/BW, mg/g	7.2±0.5	6.5±0.5	0.31
Heart weight/tibia length, mg/mm	11.7±1.1	10.2±0.8	0.27
Lung weight, wet/dry	4.6±0.3	4.9±0.2	0.44
Parasternal long axis view			
EF, %	47±1	46±1	0.57
FAC, %	32±1	30±1	0.47
EDV, μL	69±3	71±3	0.66
ESV, μL	30±2	34±3	0.38
Stroke volume, μL	30±2	29±1	0.52
Parasternal short axis view			
$EF_{Teichholz}$, %	56±1	53±3	0.44
FS, %	29±0.5	27±2	0.58
Apical 4-chamber view			
E, mm/s	729±17	739±26	0.78
A, mm/s	401±18	334±27	0.07
e′, mm/s	20±2	15±1	<0.01
a′, mm/s	16±2	17±1	0.68
E/A	1.9±0.1	2.4±0.2	0.07
E/e′	38±3	52±4	<0.01
a′/e′	0.8±0.1	1.2±0.1	0.03
IVRT, ms	19.2±0.6	22.2±0.6	<0.01
IVCT, ms	20.8±0.8	20.9±1.3	0.92
DT, ms	23.4±1.5	28.7±2.2	0.07
Tei index	0.70±0.01	0.76±0.02	0.03

Mean±SEM; n=10–12 per group; Student *t* test. ΔBW, change in body weight from baseline to final assessment; A, late diastolic filling rate; a′, late diastolic mitral annular velocity; BW, body weight; DT, deceleration time of early diastolic filling rate; E, early diastolic filling rate; e′, early diastolic mitral annular velocity; EF, ejection fraction; $EF_{Teichholz}$, EF according to Teichholz formula; FAC, fractional area change; FS, fractional shortening; EDV, end-diastolic volume; ESV, end-systolic volume; IVRT, isovolumic relaxation time; and IVCT, isovolumic contraction time. **P*<0.05; ***P*<0.01.

relation of e′ and late diastolic mitral annular velocity (**P*<0.05; Table). E/e′ ratios were significantly (***P*<0.01) increased in animals with subendocardial fibrosis (Table).

Myocardial Deformation

Myocardial strain and strain rate were assessed by speckle-tracking echocardiography in the parasternal long and short axis view (Figure 4B). In comparison to controls, isoproterenol-treated animals displayed markedly reduced global LS values (Figure 4C). Global peak radial and circumferential strain were unchanged (Figure 4C). A similar pattern was observed in strain rate, where global longitudinal strain (LS) rate declined in isoproterenol-treated animals, whereas global radial and circumferential Strain Rate remained unaffected (Figure 4C). Although LS was lowered in all myocardial segments, a significant reduction was observed in the apex of the LV only (Figure 4D).

Stress Tests

Dobutamine injections resulted in similar stress responses and did not unmask any signs of systolic dysfunction (Figure 4E; Table S3). Neither absolute peak stress values nor dobutamine-induced relative changes in echocardiographic parameters differed significantly between the 2 groups (Table S3). Similarly, no differences were observed during the graded exercise test; both groups were able to cope with comparable exercise stress in terms of covered distance and maximum running speed achieved (Figure 4F).

Diagnostic Assessment of Subendocardial Damage

Parameters with an appropriate area under the receiver operating characteristic curve for the detection of subendocardial fibrosis are displayed in Table S4. Transmural and subepicardial HA were superior predictors for subendocardial fibrosis among DT-MRI-derived parameters (Figure 5A; Table S4). Similarly, the ratio of positive to negative HA values allowed to distinguish both treatment groups (Table S4). Transmural and subendocardial MD lacked sufficient specificity, and the area under the receiver operating characteristic curve failed to reach statistical significance (Table S4). Among echocardiographic parameters, global peak LS and E/e′ were highly sensitive predictors for the presence of subendocardial fibrosis (Figure 5B; Table S4). Isovolumic relaxation time and global LS Rate also allowed to distinguish between both groups but had a remarkably lower sensitivity (Figure 5B; Table S4).

Linear regression analyses revealed clustered associations between parameters of longitudinal deformation and different DT-MRI-derived predictors for subendocardial damage (Figure 5C). Parameters of diastolic function occasionally correlated with DT-MRI measures but did not show distinct clustering (Figure 5C). Neither systolic function parameters nor radial or circumferential deformation indices showed any association (Figure 5C).

Discussion

In this experimental study, we showed that subendocardial fibrosis (1) induced changes in fiber orientation predominantly in remote regions; (2) was accompanied by signs of diastolic dysfunction and reduced longitudinal deformation, whereas systolic function and cardiac stress response remained preserved; and (3) was detectable via assessment of corresponding microstructural and functional changes.

Subendocardial Vulnerability

Metabolic demand, coronary blood supply, and compressive forces are transmurally heterogeneous where the subendocardium is at higher risk for injury than the outer layers.[1] As a consequence, several cardiovascular risk factors have been shown to affect preferentially the subendocardium during formation of cardiac organ damage (eg, hypertension,[2] diabetes mellitus,[3] ischemic heart disease,[4] and age[5]). Therefore, diagnostic markers of subendocardial status might facilitate early detection of cardiac damage, disease monitoring, and timely onset of treatment already during asymptomatic states. However, direct evidence for subendocardial pathologies is difficult to obtain in patients, and it often remains unclear whether observed changes in noninvasive surrogates are actually because of subendocardial impairment.[20–24]

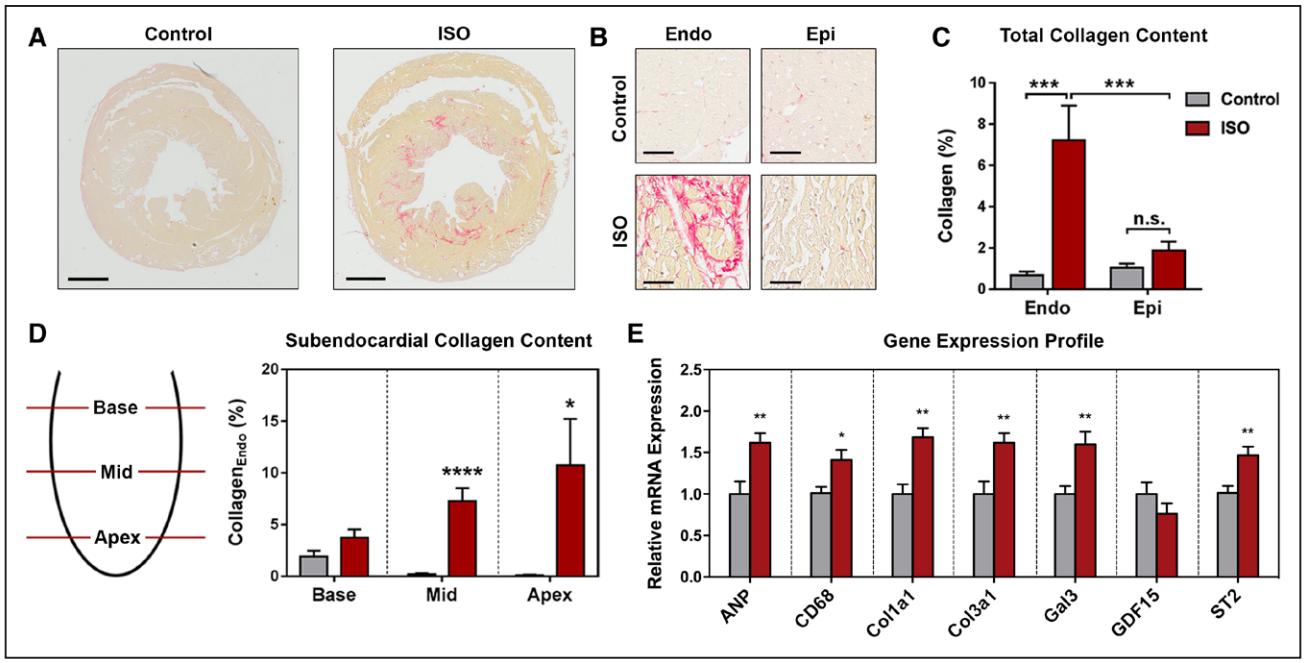

Figure 1. Cardiac tissue analyses. **A**, Representative histology of mid-myocardial cross-sections stained with picrosirius red (scale bar: 1 mm). **B**, Magnified regions within subendocardium and subepicardium (scale bar: 40 μm). **C**, Layer-specific quantification of collagen content (n=10–13 per group; 2-way ANOVA followed by Bonferroni post hoc test). **D**, Segment-specific quantification of subendocardial collagen content (n=10–13 per group; Student *t* test). **E**, Gene expression profile of the left ventricle (n=6 per group; Student *t* test). Collagen$_{Endo}$ indicates subendocardial collagen content; Endo, subendocardium; Epi, subepicardium; ISO, isoproterenol; and n.s., not significant. Mean±SEM; **P*<0.05; ***P*<0.01; ****P*<0.001; and *****P*<0.0001.

Here, we investigated an experimental model of subendocardial fibrosis in the absence of major confounders like cardiac hypertrophy or altered loading conditions,[17,18] which allowed to establish cause-effect relationships under controlled conditions. Application of isoproterenol aggravates the discrepancy between subendocardial oxygen demand and supply leading to ischemic damage in the subendocardium.[25] Accordingly, necrosis, apoptosis, and inflammatory pathways may have contributed to the observed phenotype, as well as differences in calcium signaling, coronary microcirculation, and membrane permeability.[25] The presence of CD68$^+$ cells 2 weeks after final isoproterenol treatment indicates that sustained immune response may also play a role.

Isoproterenol acts via β-adrenergic receptors, whose density is highest at the apex of the LV.[26] Accordingly, damage in this model is predominantly located in apical regions, as shown before.[27]

Microstructural Changes in Response to Subendocardial Damage

Our understanding of structural-functional relationships in the heart is incomplete.[28] DT-MRI is a feasible tool to study the 3-dimensional myofiber arrangement that has been applied in various cardiovascular pathologies in both experimental models[9,15,16,19] and patients.[10,14,29] Despite the growing wealth of cardiac DT-MRI studies, however, there is a lack of data regarding changes that occur during early disease states and investigation of layer-specific alterations.[30] Additionally, the sequential morphological and functional changes during transition from initial subendocardial damage to transmural affection are largely unclear. To our knowledge, this is the first application of DT-MRI to characterize the impact of subendocardial damage on myocardial microstructure.

The effect of fibrosis on MD and FA is controversial.[9,29,31] Subendocardial scarring was accompanied by decreased MD and unaltered FA, which is in accordance with a study by Wu et al[9] that showed decreased subendocardial MD but unchanged transmural FA in the scar tissue after myocardial infarction. Similarly, Strijkers et al[31] reported on reduced MD and increased FA in the infarct region. In contrast, other studies attributed myocardial fibrosis to increased MD and decreased FA.[29,32] This implies that changes in MD might be a promising, yet nonspecific marker for myocardial fibrosis and that future studies are needed to identify morphological correlates for changes in these parameters under different pathological conditions.

In general, MD is considered to decrease with increased cellularity or reduced extracellular space, respectively. Isoproterenol-treatment is known to induce cardiomyocyte hypertrophy and collagen deposition that fills major parts of the extracellular space,[33] both conditions in which free extracellular space is reduced. We, therefore, hypothesize that the observed decline in MD might be due to the relative loss of extracellular space and the consecutive slower diffusion of water molecules in this particular model.

It has been shown that residual myofibers serve as a scaffold for newly developing collagen fiber tracts during scar formation, and that these collagen fibers have the same orientation as surrounding myofibers.[34] FA is considered a measure of directional coherence and orientational integrity. Accordingly, such structured collagen fibers may account for observed unaltered FA in case of no greater disturbance of tissue organization.

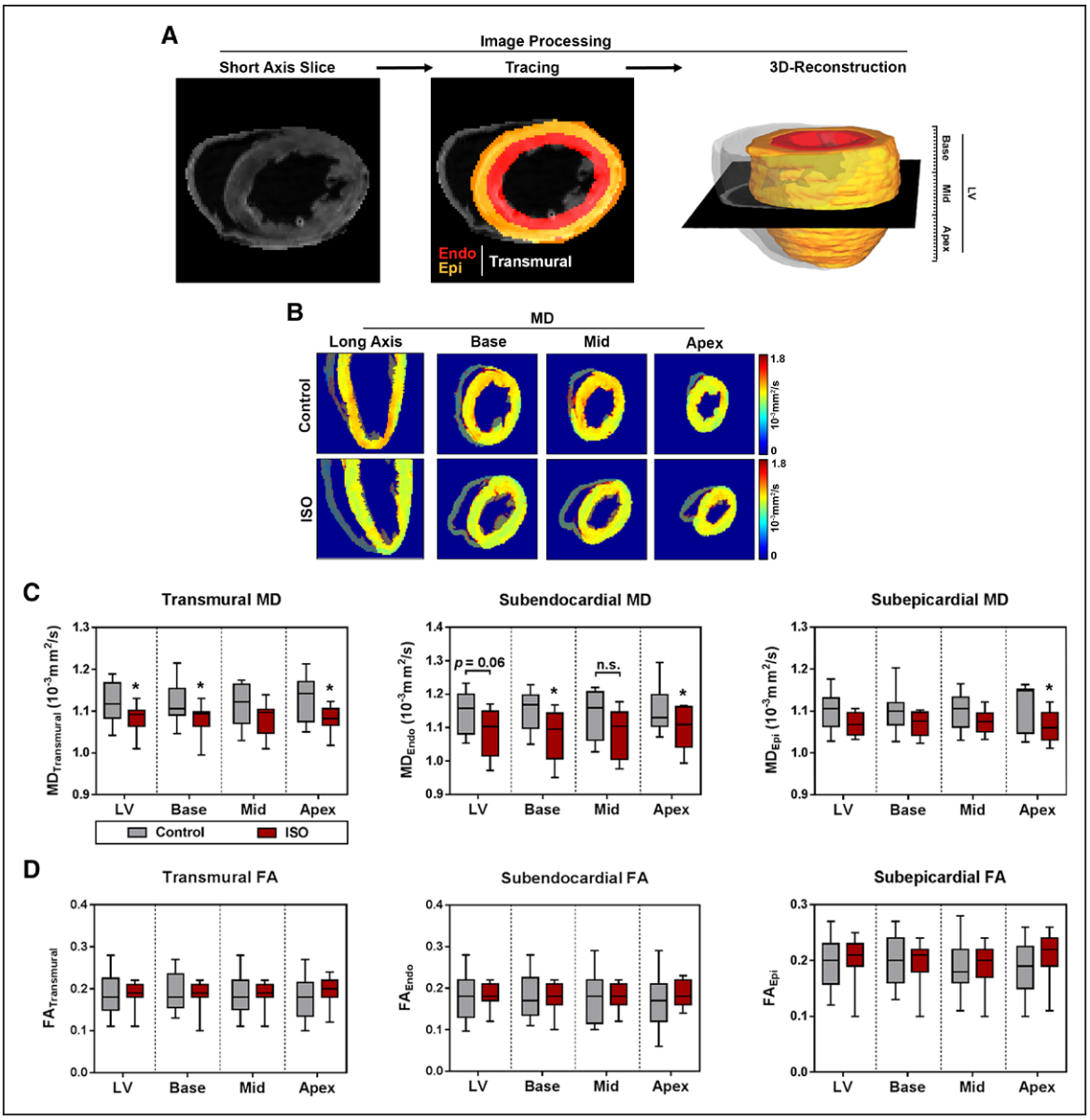

Figure 2. Diffusion tensor magnetic resonance imaging post-processing and diffusion metrics. **A**, Endocardial and epicardial borders were traced manually in multiple short axis slices per heart, and subendocardium (Endo) and subepicardium (Epi) were defined as regions of interest. Subsequently, 3-dimensional volumes were rendered by tomographic reconstruction allowing analyses of both regions for the whole left ventricle (LV) or within myocardial segments (base/mid/apex). **B**, Representative color maps for mean diffusivity (MD) in a reconstructed cardiac long axis and different myocardial short axis segments. **C**, Analysis of MD. **D**, Analysis of fractional anisotropy (FA). Medians and quartiles with minimum and maximum values; n=9–11 per group; Student *t* test. **P*<0.05. ISO indicates isoproterenol.

Notably, no changes in the subendocardial HA were observed despite histological proof of subendocardial fibrotic lesions. Again, formation of collagen fibers running in parallel to residual myofiber tracts[34] may be a likely explanation. In contrast to complete coronary occlusion, scarring in this model occurs next to viable myofiber tracts, and damage is limited to the subendocardium. As a putative mechanism, newly formed collagen fibers may have the same orientation as surrounding myofibers and the ones they replace in response to damage. In the latter case, no greater changes in HA may be detectable.

Subendocardial fibrosis was accompanied by a left shift in HA towards lower values, which is present also in other pathologies.[11,14,16] Interestingly, this left-shift was caused predominantly by subepicardial but not subendocardial myofibers. This suggests that circumscribed subendocardial damage affects also remote regions and induces microstructural remodeling within the entire LV. Similarly, microstructural changes in response to myocardial infarction also involve the remote zone, in which a left shift in HA can be observed.[9] It remains unclear whether this represents adaptive reorientation or passive mechanisms, and further studies are required to clarify the biological relevance of these findings.

Functional Changes in Response to Subendocardial Damage

Isolated subendocardial damage resulted in a phenotype resembling several hallmarks of cardiovascular high-risk patients in the absence of heart failure symptoms or signs. Since

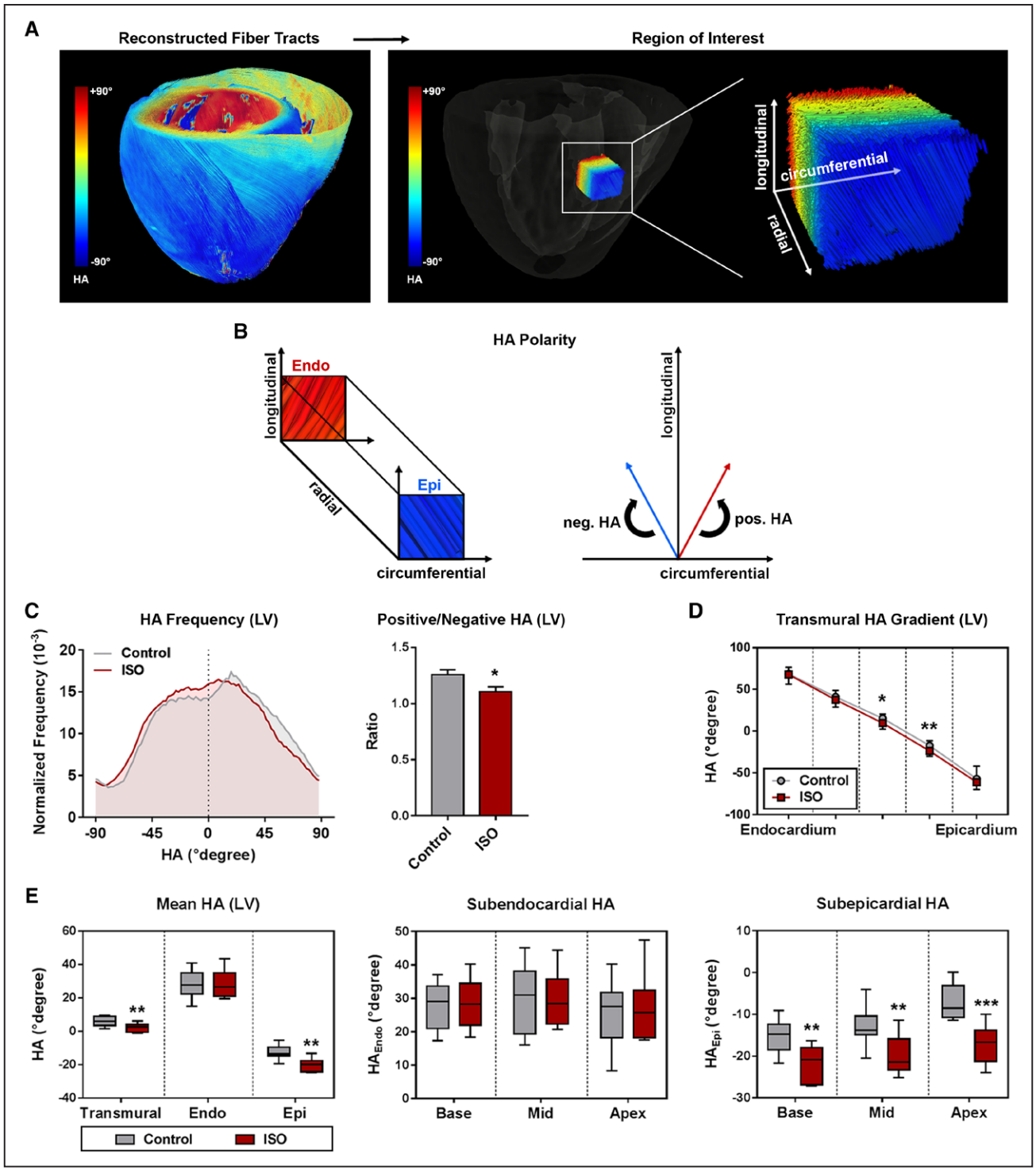

Figure 3. Myofiber geometry. **A**, Representative reconstruction of fiber tracts: helix angle (HA) in the left ventricle (LV) changes continuously from positive values in the subendocardium (right-handed helix), over neutral in the mesocardium, to negative values in the subepicardium (left-handed helix). **B**, Definition of HA-polarity. Mean±SEM (**C**, **D**) or medians and quartiles with minimum and maximum values. **E**, Analysis of HA. Medians and quartiles with minimum and maximum values; n=9–11 per group; Student *t* test. Endo indicates subendocardium; Epi, subepicardium; and ISO, isoproterenol. **P*<0.05 and ***P*<0.01.

impairment of either subendocardium, subepicardium, or transmural myocardium results in distinct phenotypes, it has been proposed to classify heart failure according to the damaged myocardial layer(s).[35,36] Selective subendocardial involvement is usually considered a marker of subclinical disease,[1] which may be accompanied by diastolic dysfunction but preserved ejection fraction together with reduced longitudinal but unaltered radial and circumferential mechanics in patients.[36] The experimental model we used demonstrated a comparable phenotype, which provides evidence for corresponding classification.

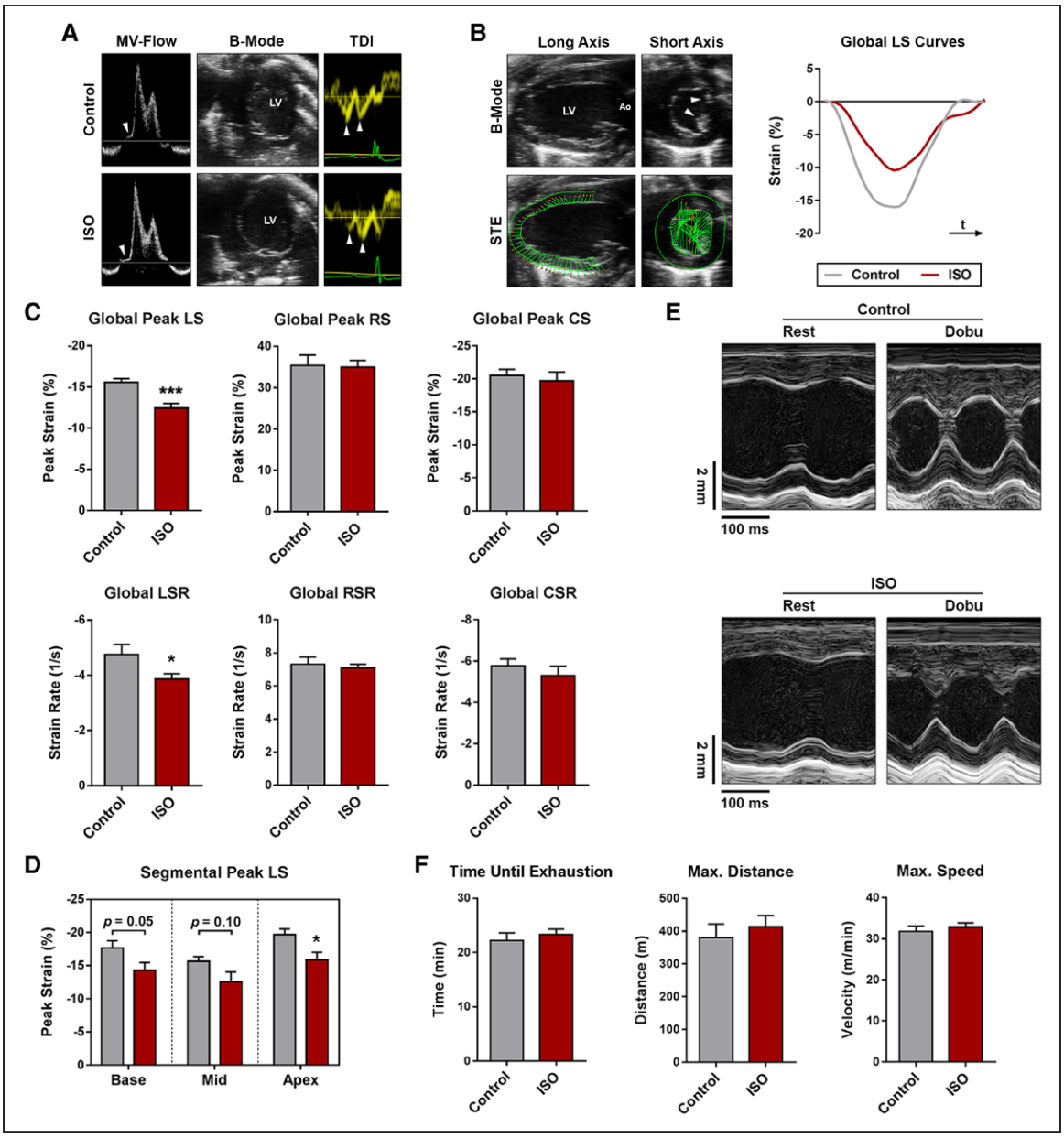

Figure 4. Functional analyses. **A**, Representative transmitral flow patterns (**left**; arrows indicate isovolumic relaxation time), B-mode images of the apical 4 chamber view (**mid**), and tissue Doppler analyses of the septal mitral annulus (**right**; arrows indicate early and late diastolic mitral annular velocities). **B**, Speckle-tracking echocardiography and representative longitudinal strain (LS) curves over one cardiac cycle (arrows indicate papillary muscles). **C**, Global peak strain and global strain rate. **D**, Segmental peak LS. **E**, Representative M-mode images acquired in the parasternal short axis view at rest and during Dobu stress. **F**, Results of the graded exercise test protocol. n=7–12 per group; Student *t* test. Ao indicates aorta; Col1a1, collagen type I, alpha 1 chain; Col3a1, collagen type III, alpha 1 chain; $Collagen_{Endo}$, subendocardial collagen content; CS, circumferential strain; CSR, circumferential strain rate; Dobu, dobutamine; ISO, isoproterenol; LSR, longitudinal strain rate; LV, left ventricle; MV-Flow, transmitral flow pattern; RS, radial strain; RSR, radial strain rate; STE, speckle-tracking echocardiography; and TDI, tissue Doppler imaging. Mean±SEM; **P*<0.05 and ****P*<0.001.

Animals with subendocardial fibrosis showed mild diastolic dysfunction, suggesting that isolated subendocardial fibrosis alone may account for preclinical diastolic dysfunction. As such, subendocardial fibrosis may be of considerable relevance given that preclinical diastolic dysfunction has been shown to be highly prevalent in large population-based studies and that a relevant portion of these subjects shows a progression to congestive heart failure over time.[37,38] Our findings are supported by clinical studies reporting on preclinical diastolic dysfunction in asymptomatic patients with risk factors that are known to affect preferentially the subendocardium.[21,22] However, these studies relied on nonspecific surrogates and did not provide direct evidence for subendocardial pathologies, which warrants further investigations in patients with confirmed subendocardial damage.

Longitudinal, yet not radial or circumferential deformation declined in animals with subendocardial fibrosis. Reduced LS is a common feature of both high-risk patients[21–24] and subjects with overt heart failure. Since longitudinal mechanics of the LV are determined mainly by subendocardial myofibers, impaired LS parameters are well-accepted surrogates of putative subendocardial damage.[1] Reduced LS has been linked

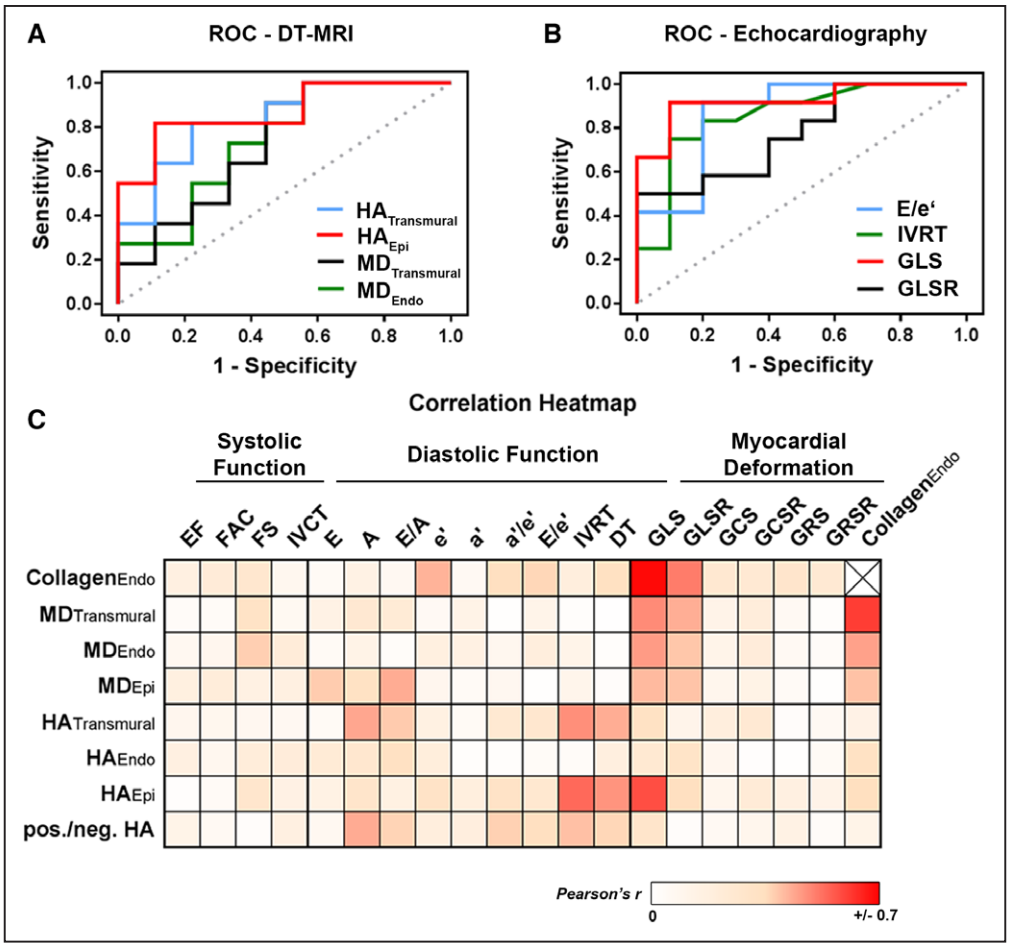

Figure 5. Receiver operating characteristic (ROC) curves and correlation analyses. **A**, ROC curves for diffusion tensor magnetic resonance imaging (DT-MRI)-derived parameters to detect subendocardial fibrosis. **B**, ROC curves for echocardiographic parameters to detect subendocardial fibrosis. **C**, Color-coded correlation coefficients of various parameters (Pearson correlation coefficient *r*). A indicates late diastolic filling rate; a′, late diastolic mitral annular velocity; DT, deceleration time of early diastolic filling rate; E, early diastolic filling rate; e′, early diastolic mitral annular velocity; EF, ejection fraction; FAC, fractional area change; FS, fractional shortening; GCS, global peak circumferential strain; GCRS, global circumferential strain rate; GLS, global peak longitudinal strain; GLSR, global longitudinal strain rate; GRS, global peak radial strain; GRSR, global radial strain rate; HA_{Epi}, subepicardial helix angle; HA_{Endo}, subendocardial helix angle; $HA_{Transmural,}$ transmural helix angle; IVCT, isovolumic contraction time; IVRT, isovolumic relaxation time; MD_{Epi}, subepicardial mean diffusivity; MD_{Endo}, subendocardial mean diffusivity; and $MD_{Transmural}$, transmural mean diffusivity.

to subendocardial fibrosis in preclinical patients due to correlations with circulating biomarkers of increased extracellular matrix turnover.[20,21] Our results confirm that reduced longitudinal deformation indeed closely reflects subendocardial fibrosis, and that global peak LS can serve for diagnostic assessment. This is in accordance with previous studies in this model[18] and in experimental hypertensive heart disease.[2]

Biomarkers play a pivotal role in the clinical diagnosis of heart failure, and several studies demonstrated that circulating markers of cell damage, extracellular matrix turnover, and inflammation are elevated in these patients.[39] We found that several biomarkers associated with heart failure were upregulated in the LV of animals presenting with isolated subendocardial fibrosis. This might be of interest for future studies regarding biomarker assessment in preclinical high-risk patients.

Limitations

The isoproterenol-model is limited with regards to the comparability of the human situation, and technical issues of small animal echocardiography (eg, susceptibility to off-axis imaging, spatial/temporal resolution, and assessment under anesthesia) should be considered. Myocardial deformation analysis by speckle-tracking echocardiography in small animals is limited regarding assessment of left-ventricular torsion. The latter may be assessed by magnetic resonance imaging, which, however, was performed ex vivo in our study, and thus did not allow to study dynamic changes occurring during the cardiac cycle. The model we used is known to develop elevated diastolic pressures,[40] and we observed increased E/e′ ratios as a noninvasive surrogate. However, invasive measurements of hemodynamics were not performed in the present study. We applied an established graded exercise test protocol that was originally developed for another mouse strain,[41] and that has never been evaluated in 129/Sv mice before. Due to technical issues, only systolic function parameters could have been assessed during dobutamine stress. Biomarker expression was determined 2 weeks after final treatment with isoproterenol. Despite this relatively long time period, direct action of isoproterenol on biomarker expression cannot be ruled out. There was no readout for successful cardioplegic arrest, and fixation during different phases of the cardiac cycle may have an impact on DT-MRI analyses. Hearts were scanned after

comparable time intervals of fixation, but absolute values of MD and FA might have been affected by formalin-fixation.[42]

Conclusions

Circumscribed subendocardial damage can account for several hallmarks observed in cardiovascular high-risk patients. Microstructural remodeling in response to subendocardial damage involves also other myocardial layers indicating a newly identified remote process.

Finally, our data provide translational evidence for both established surrogates of subendocardial damage and novel markers of microstructural remodeling that might serve as diagnostic measures for early detection of cardiac impairment. Among these, global peak LS and subepicardial HA were the best predictors of subendocardial damage.

Perspectives

As a future direction, DT-MRI may be used to identify characteristic microstructural changes in various cardiac diseases facilitating diagnostic application. Based on this, DT-MRI might help to further improve our understanding of cardiac pathologies and might ultimately serve as a diagnostic tool in patients. The present work indicates that microstructural changes are present already in early disease stages, and that DT-MRI is capable of assessing them. These findings have to be confirmed in patients by in vivo DT-MRI for translation of our results. The transmural heterogeneity of microstructural changes as observed in our study should be considered in future investigations.

Acknowledgments

We thank Beata Höft for her excellent technical assistance, Moritz Fischer for the help in designing the DT-MRI setup, Franziska Schwarz (scivisto.com) for the graphical abstract, and Andrew D. Scott (Royal Brompton Hospital and Imperial College London) for insightful discussions regarding the DT-MRI data. Parts of this work will be used in the doctoral thesis of David Lohr.

Sources of Funding

This work was supported by the German Centre for Cardiovascular Research (DZHK; BER 5.4 PR) and by the German Ministry of Education and Research (grant numbers 01EO1004 and 01EO1504). Arne Thiele is supported by a research grant of the German cardiac society (DGK).

Disclosures

None.

References

1. Stanton T, Marwick TH. Assessment of subendocardial structure and function. *JACC Cardiovasc Imaging.* 2010;3:867–875. doi: 10.1016/j.jcmg.2010.05.011
2. Ishizu T, Seo Y, Kameda Y, Kawamura R, Kimura T, Shimojo N, Xu D, Murakoshi N, Aonuma K. Left ventricular strain and transmural distribution of structural remodeling in hypertensive heart disease. *Hypertension.* 2014;63:500–506. doi: 10.1161/HYPERTENSIONAHA.113.02149
3. Martinez DA, Guhl DJ, Stanley WC, Vailas AC. Extracellular matrix maturation in the left ventricle of normal and diabetic swine. *Diabetes Res Clin Pract.* 2003;59:1–9.
4. Bache RJ, Schwartz JS. Effect of perfusion pressure distal to a coronary stenosis on transmural myocardial blood flow. *Circulation.* 1982;65:928–935. doi: 10.1161/01.CIR.65.5.928
5. Wanagat J, Wolff MR, Aiken JM. Age-associated changes in function, structure and mitochondrial genetic and enzymatic abnormalities in the Fischer 344 x Brown Norway F(1) hybrid rat heart. *J Mol Cell Cardiol.* 2002;34:17–28. doi: 10.1006/jmcc.2001.1483
6. Harrison DG, Florentine MS, Brooks LA, Cooper SM, Marcus ML. The effect of hypertension and left ventricular hypertrophy on the lower range of coronary autoregulation. *Circulation.* 1988;77:1108–1115. doi: 10.1161/01.CIR.77.5.1108
7. Fujii M, Nuno DW, Lamping KG, Dellsperger KC, Eastham CL, Harrison DG. Effect of hypertension and hypertrophy on coronary microvascular pressure. *Circ Res.* 1992;71:120–126.
8. Mor-Avi V, Lang RM, Badano LP, et al. Current and evolving echocardiographic techniques for the quantitative evaluation of cardiac mechanics: ASE/EAE consensus statement on methodology and indications endorsed by the Japanese Society of Echocardiography. *J Am Soc Echocardiogr.* 2011;24:277–313. doi: 10.1016/j.echo.2011.01.015
9. Wu Y, Zhang LJ, Zou C, Tse HF, Wu EX. Transmural heterogeneity of left ventricular myocardium remodeling in postinfarct porcine model revealed by MR diffusion tensor imaging. *J Magn Reson Imaging.* 2011;34:43–49. doi: 10.1002/jmri.22589
10. Nielles-Vallespin S, Khalique Z, Ferreira PF, et al. Assessment of myocardial microstructural dynamics by *in vivo* diffusion tensor cardiac magnetic resonance. *J Am Coll Cardiol.* 2017;69:661–676. doi: 10.1016/j.jacc.2016.11.051
11. von Deuster C, Sammut E, Asner L, Nordsletten D, Lamata P, Stoeck CT, Kozerke S, Razavi R. Studying dynamic myofiber aggregate reorientation in dilated cardiomyopathy using in vivo magnetic resonance diffusion tensor imaging. *Circ Cardiovasc Imaging*. 2016;9:e005018. doi: 10.1161/CIRCIMAGING.116.005018
12. Streeter DD Jr, Spotnitz HM, Patel DP, Ross J Jr, Sonnenblick EH. Fiber orientation in the canine left ventricle during diastole and systole. *Circ Res.* 1969;24:339–347. doi: 10.1161/01.RES.24.3.339
13. Palit A, Bhudia SK, Arvanitis TN, Turley GA, Williams MA. Computational modelling of left-ventricular diastolic mechanics: effect of fibre orientation and right-ventricle topology. *J Biomech.* 2015;48:604–612. doi: 10.1016/j.jbiomech.2014.12.054
14. Wu MT, Tseng WY, Su MY, Liu CP, Chiou KR, Wedeen VJ, Reese TG, Yang CF. Diffusion tensor magnetic resonance imaging mapping the fiber architecture remodeling in human myocardium after infarction: correlation with viability and wall motion. *Circulation.* 2006;114:1036–1045. doi: 10.1161/CIRCULATIONAHA.105.545863
15. Sosnovik DE, Mekkaoui C, Huang S, Chen HH, Dai G, Stoeck CT, Ngoy S, Guan J, Wang R, Kostis WJ, Jackowski MP, Wedeen VJ, Kozerke S, Liao R. Microstructural impact of ischemia and bone marrow-derived cell therapy revealed with diffusion tensor magnetic resonance imaging tractography of the heart in vivo. *Circulation.* 2014;129:1731–1741. doi: 10.1161/CIRCULATIONAHA.113.005841
16. Wu EX, Wu Y, Nicholls JM, Wang J, Liao S, Zhu S, Lau CP, Tse HF. MR diffusion tensor imaging study of postinfarct myocardium structural remodeling in a porcine model. *Magn Reson Med.* 2007;58:687–695. doi: 10.1002/mrm.21350
17. Samuel CS, Bodaragama H, Chew JY, Widdop RE, Royce SG, Hewitson TD. Serelaxin is a more efficacious antifibrotic than enalapril in an experimental model of heart disease. *Hypertension.* 2014;64:315–322. doi: 10.1161/HYPERTENSIONAHA.114.03594
18. Beyhoff N, Brix S, Betz IR, Klopfleisch R, Foryst-Ludwig A, Krannich A, Stawowy P, Knebel F, Grune J, Kintscher U. Application of speckle-tracking echocardiography in an experimental model of isolated subendocardial damage. *J Am Soc Echocardiogr.* 2017;30:1239.e2–1250.e2. doi: 10.1016/j.echo.2017.08.006
19. Lohr D, Terekhov M, Weng AM, Schroeder A, Walles H, Schreiber LM. Spin echo based cardiac diffusion imaging at 7T: an ex vivo study of the porcine heart at 7T and 3T. *PLoS One.* 2019;14:e0213994. doi: 10.1371/journal.pone.0213994
20. Ikonomidis I, Tzortzis S, Triantafyllidi H, Parissis J, Papadopoulos C, Venetsanou K, Trivilou P, Paraskevaidis I, Lekakis J. Association of impaired left ventricular twisting-untwisting with vascular dysfunction, neurohumoral activation and impaired exercise capacity in hypertensive heart disease. *Eur J Heart Fail.* 2015;17:1240–1251. doi: 10.1002/ejhf.403
21. Kang SJ, Lim HS, Choi BJ, Choi SY, Hwang GS, Yoon MH, Tahk SJ, Shin JH. Longitudinal strain and torsion assessed by two-dimensional speckle tracking correlate with the serum level of tissue inhibitor of matrix metalloproteinase-1, a marker of myocardial fibrosis, in patients with hypertension. *J Am Soc Echocardiogr.* 2008;21:907–911. doi: 10.1016/j.echo.2008.01.015

22. Mizuguchi Y, Oishi Y, Miyoshi H, Iuchi A, Nagase N, Oki T. The functional role of longitudinal, circumferential, and radial myocardial deformation for regulating the early impairment of left ventricular contraction and relaxation in patients with cardiovascular risk factors: a study with two-dimensional strain imaging. *J Am Soc Echocardiogr.* 2008;21:1138–1144. doi: 10.1016/j.echo.2008.07.016
23. Parikh JD, Hollingsworth KG, Wallace D, Blamire AM, MacGowan GA. Normal age-related changes in left ventricular function: role of afterload and subendocardial dysfunction. *Int J Cardiol.* 2016;223:306–312. doi: 10.1016/j.ijcard.2016.07.252
24. Lumens J, Delhaas T, Arts T, Cowan BR, Young AA. Impaired subendocardial contractile myofiber function in asymptomatic aged humans, as detected using MRI. *Am J Physiol Heart Circ Physiol.* 2006;291:H1573–H1579. doi: 10.1152/ajpheart.00074.2006
25. Rona G. Catecholamine cardiotoxicity. *J Mol Cell Cardiol.* 1985;17:291–306. doi: 10.1016/S0022-2828(85)80130-9
26. Mori H, Ishikawa S, Kojima S, Hayashi J, Watanabe Y, Hoffman JI, Okino H. Increased responsiveness of left ventricular apical myocardium to adrenergic stimuli. *Cardiovasc Res.* 1993;27:192–198. doi: 10.1093/cvr/27.2.192
27. Collins P, Billings CG, Barer GR, Daly JJ, Jolly A. Quantitation of isoprenaline-induced changes in the ventricular myocardium. *Cardiovasc Res.* 1975;9:797–806. doi: 10.1093/cvr/9.6.797
28. Buckberg GD, Weisfeldt ML, Ballester M, et al. Left ventricular form and function: scientific priorities and strategic planning for development of new views of disease. *Circulation.* 2004;110:e333–e336. doi: 10.1161/01.CIR.0000143625.56882.5C
29. Abdullah OM, Drakos SG, Diakos NA, Wever-Pinzon O, Kfoury AG, Stehlik J, Selzman CH, Reid BB, Brunisholz K, Verma DR, Myrick C, Sachse FB, Li DY, Hsu EW. Characterization of diffuse fibrosis in the failing human heart via diffusion tensor imaging and quantitative histological validation. *NMR Biomed.* 2014;27:1378–1386. doi: 10.1002/nbm.3200
30. Watson SR, Dormer JD, Fei B. Imaging technologies for cardiac fiber and heart failure: a review. *Heart Fail Rev.* 2018;23:273–289. doi: 10.1007/s10741-018-9684-1
31. Strijkers GJ, Bouts A, Blankesteijn WM, Peeters TH, Vilanova A, van Prooijen MC, Sanders HM, Heijman E, Nicolay K. Diffusion tensor imaging of left ventricular remodeling in response to myocardial infarction in the mouse. *NMR Biomed.* 2009;22:182–190. doi: 10.1002/nbm.1299
32. Pop M, Ghugre NR, Ramanan V, Morikawa L, Stanisz G, Dick AJ, Wright GA. Quantification of fibrosis in infarcted swine hearts by ex vivo late gadolinium-enhancement and diffusion-weighted MRI methods. *Phys Med Biol.* 2013;58:5009–5028. doi: 10.1088/0031-9155/58/15/5009
33. Pick R, Jalil JE, Janicki JS, Weber KT. The fibrillar nature and structure of isoproterenol-induced myocardial fibrosis in the rat. *Am J Pathol.* 1989;134:365–371.
34. Goergen CJ, Chen HH, Sakadžić S, Srinivasan VJ, Sosnovik DE. Microstructural characterization of myocardial infarction with optical coherence tractography and two-photon microscopy. *Physiol Rep.* 2016;4:e12894. doi: 10.14814/phy2.12894
35. Sengupta PP, Narula J. Reclassifying heart failure: predominantly subendocardial, subepicardial, and transmural. *Heart Fail Clin.* 2008;4:379–382. doi: 10.1016/j.hfc.2008.03.013
36. Geyer H, Caracciolo G, Abe H, Wilansky S, Carerj S, Gentile F, Nesser HJ, Khandheria B, Narula J, Sengupta PP. Assessment of myocardial mechanics using speckle tracking echocardiography: fundamentals and clinical applications. *J Am Soc Echocardiogr.* 2010;23:351–369; quiz 453. doi: 10.1016/j.echo.2010.02.015
37. Kane GC, Karon BL, Mahoney DW, Redfield MM, Roger VL, Burnett JC Jr, Jacobsen SJ, Rodeheffer RJ. Progression of left ventricular diastolic dysfunction and risk of heart failure. *JAMA.* 2011;306:856–863. doi: 10.1001/jama.2011.1201
38. Vogel MW, Slusser JP, Hodge DO, Chen HH. The natural history of preclinical diastolic dysfunction: a population-based study. *Circ Heart Fail.* 2012;5:144–151. doi: 10.1161/CIRCHEARTFAILURE.110.959668
39. de Boer RA, Daniels LB, Maisel AS, Januzzi JL Jr. State of the art: newer biomarkers in heart failure. *Eur J Heart Fail.* 2015;17:559–569. doi: 10.1002/ejhf.273
40. Brooks WW, Conrad CH. Isoproterenol-induced myocardial injury and diastolic dysfunction in mice: structural and functional correlates. *Comp Med.* 2009;59:339–343.
41. Petrosino JM, Heiss VJ, Maurya SK, Kalyanasundaram A, Periasamy M, LaFountain RA, Wilson JM, Simonetti OP, Ziouzenkova O. Graded maximal exercise testing to assess mouse cardio-metabolic phenotypes. *PLoS One.* 2016;11:e0148010. doi: 10.1371/journal.pone.0148010
42. Giannakidis A, Gullberg GT, Pennell DJ, Firmin DN. Value of formalin fixation for the prolonged preservation of rodent myocardial microanatomical organization: evidence by MR diffusion tensor imaging. *Anat Rec (Hoboken).* 2016;299:878–887. doi: 10.1002/ar.23359

Novelty and Significance

What Is New?

- First characterization of microstructural changes in response to subendocardial damage by diffusion tensor magnetic resonance imaging.
- Comprehensive assessment of functional consequences of isolated subendocardial damage in the absence of confounding factors.

What Is Relevant?

- Subendocardial damage leads to microstructural reorganization of cardiac fibers predominantly in remote regions.
- Subendocardial damage can account for several observations in cardiovascular high-risk patients, and assessment of corresponding changes may facilitate early detection of cardiac damages.

Summary

Isolated subendocardial damage resulted in a phenotype resembling several hallmarks of cardiovascular high-risk patients, and changes in myofiber arrangement under these conditions were characterized for the first time.